

Throughput Optimization of Intelligent Reflecting Surface Assisted User Cooperation in WPCNs

Yuan Zheng*, Suzhi Bi*[†], Ying-Jun Angela Zhang[‡], and Hui Wang*

*College of Electronic and Information Engineering, Shenzhen University, Shenzhen, 518060, China

[†]Peng Cheng Laboratory, Shenzhen, 518066, China

[‡]Department of Information Engineering, The Chinese University of Hong Kong, Shatin, N.T., Hong Kong SAR

E-mail: *{zhyu, bsz, wanghsz}@szu.edu.cn, [‡]yjzhang@ie.cuhk.edu.hk

Abstract—Intelligent reflecting surface (IRS) can effectively enhance the energy and spectral efficiency of wireless communication system through the use of a large number of low-cost passive reflecting elements. In this paper, we investigate throughput optimization of IRS-assisted user cooperation in a wireless powered communication network (WPCN), where the two WDs harvest wireless energy and transmit information to a common hybrid access point (HAP). In particular, the two WDs first exchange their independent information with each other and then form a virtual antenna array to transmit jointly to the HAP. We aim to maximize the common (minimum) throughput performance by jointly optimizing the transmit time and power allocations of the two WDs on wireless energy and information transmissions and the passive array coefficients on reflecting the wireless energy and information signals. By comparing with some existing benchmark schemes, our results show that the proposed IRS-assisted user cooperation method can effectively improve the throughput performance of cooperative transmission in WPCNs.

I. INTRODUCTION

To meet the increasing device energy consumption of modern wireless networks, wireless powered communication network (WPCN) has been recently proposed and widely studied (e.g., [1]–[5]), which uses dedicated wireless energy transferring nodes to power the operation of communication devices. Compared to its conventional battery-powered counterpart, WPCN has shown its advantages in lowering the network operating cost and improving the robustness of communication service especially in low power applications, such as sensor and internet of things (IoT) networks. The major technical challenge in WPCNs is the low power transfer efficiency over long distance, which also leads to severe user unfairness problem in the achievable data rates due to the dissimilar user locations. To tackle the user unfairness problem, many user cooperation methods have been proposed and have demonstrated their effectiveness in various network setups [6]–[9]. Nonetheless, the low energy transfer efficiency is still a fundamental performance bottleneck of WPCN systems.

Recently, with the developments in meta-surface technology [10], intelligent reflecting surface (IRS) technology has received widespread attention in wireless communications [11]. In particular, an IRS comprises a massive number of reconfigurable reflecting elements and a smart controller, where each element can reflect impinging electromagnetic waves with a controllable phase shift using the IRS controller. By properly

adjusting the phase shifts of the elements of IRS, the reflected signals can be coherently combined with those from other paths at the receiver to maximize the signal strength. Combining the virtual array gain and the reflect beamforming gain, the IRS is capable of enhancing wireless energy transfer efficiency and therefore fulfilling the potential of WPCNs.

Previous studies have reported the application of the IRS in wireless communications [12]–[15]. For instance, [12] considered a joint design of active beamforming at the base station (BS) and passive beamforming at the IRS to minimize the total transmit power. [13] studied the transmit power allocation and passive beamforming design to maximize energy/spectral efficiency. [14] proposed to use a set of distributed IRSs to assist simultaneous wireless information and power transfer (SWIPT) from a multi-antenna AP to multiple information receivers and energy receivers. Multiple-input multiple-output (MIMO) beamforming was investigated in [15] for IRS-assisted systems, where the phase shifts were either given or designed only for rank-one BS-to-IRS line-of-sight (LOS) channel. However, most of the existing works only exploit IRS for enhancing the received signal strength in the forward links (FLs) from the BS to the users. In practice, the reflection of IRS is also applicable to improve the spectral efficiency in the reverse links (RLs).

In this paper, we investigate a novel IRS-assisted two-user cooperation method in WPCNs. As shown in Fig. 1, we consider that an HAP broadcasts wireless energy to two WDs in the FLs and receives cooperative information transmission in the RLs. Specifically, the two WDs first exchange their independent information with each other and then form a virtual antenna array to transmit jointly to the HAP. In this case, the IRS is used to assist the wireless energy transfer (WET), the information exchange among the two WDs, and the joint wireless information transmission (WIT) to the HAP. With the proposed IRS-assisted cooperation method, we formulate an optimization problem to maximize the common throughput of the two users, which is an important metric of user fairness in WPCN. This involves a joint optimization of the transmit time, power allocation of the two WDs on wireless energy and information transmissions, and the passive array coefficients to reflect the wireless energy and information signals. We propose an efficient method to tackle the non-

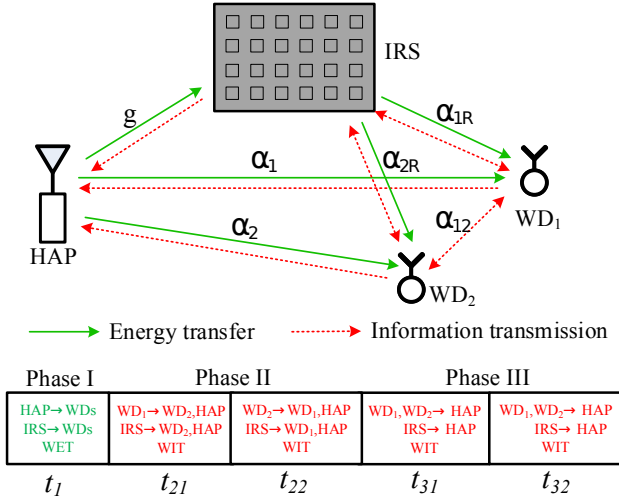


Fig. 1. The network structure and transmit protocol of the proposed IRS-assisted cooperation scheme.

convex problem. Besides, we conduct extensive simulations to show that the proposed IRS-assisted method can effectively enhance the throughput performance in WPCN compared with some representative benchmark methods.

II. SYSTEM MODEL

A. Channel Model

As show in Fig. 1, we consider a WPCN consisting of one HAP and two WDs denoted by WD_1 and WD_2 , where the HAP and WDs have a single antenna each. Both WDs first harvest RF energy in the FL and then transmit information in the RL. To enhance the propagation performance, we employ an IRS composed of N passive elements in the vicinity of the devices to assist the transmissions of the WPCN. The IRS can dynamically adjust the phase shift of each reflecting element based on the propagation environment learned through periodic sensing. Due to the substantial path loss, we only consider one-time signal reflection by the IRS and ignore the signals that are reflected thereafter.

For simplicity, we assume that all channels experience quasi-static flat fading and follow channel reciprocity between the FL and RL. The baseband equivalent channels from the HAP to IRS, from IRS to WD_i , from the HAP to WD_i and from WD_1 to WD_2 are denoted by $\mathbf{g} \in \mathbb{C}^{1 \times N}$, $\alpha_{iR} \in \mathbb{C}^{N \times 1}$, $i = 1, 2$, α_i and α_{12} , respectively. We denote $g = \|\mathbf{g}\|^2$, $h_{iR} = \|\alpha_{iR}\|^2$, $h_i = |\alpha_i|^2$ and $h_{12} = |\alpha_{12}|^2$ as the corresponding channel gains. It is assumed that the channels of different transceiver pairs are independent to each other. Besides, the entries inside all channel vectors are modeled as zero-mean independent and identically distributed (i.i.d.) complex Gaussian random variables with variance depending on the path loss of the respective wireless links. We denote $\Theta = \text{diag}(\beta_1 v_1, \dots, \beta_N v_N, \dots, \beta_N v_N)$ with $v_n = e^{j\theta_n}$, $n = 1, \dots, N$ as the diagonal reflection coefficient matrix at the IRS, where $\beta_n \in [0, 1]$ and $\theta_n \in [0, 2\pi]$ are the amplitude coefficient and phase shift of each element, respectively ($\text{diag}(\mathbf{a})$

denotes a diagonal matrix with its diagonal elements given in the vector \mathbf{a}). We assume that both the HAP and IRS have perfect channel state information (CSI) like in [12]–[16].

B. Protocol Description

As shown in Fig. 1, we consider a three-phase operating protocol of the proposed scheme. In the first phase of duration t_1 , the HAP transfers wireless energy in the FL for the two WDs to harvest. Meanwhile, the IRS scatters the incident signal from the HAP to the WDs, such that the WDs receive both the direct-path and reflect-path signals from the HAP. In the second phase of duration t_{21} and t_{22} , WD_1 and WD_2 exchange their information to each other with the help of IRS. In the last phase of length t_3 , WD_1 and WD_2 jointly transmit their information to the HAP with the help of IRS. Specifically, the two WDs first jointly transmit the information of WD_1 and then the information of WD_2 with duration t_{31} and t_{32} , respectively, with $t_3 = t_{31} + t_{32}$. Note that we have a total time constraint

$$t_1 + t_{21} + t_{22} + t_{31} + t_{32} \leq T. \quad (1)$$

As no inter-user interference exists in the above mentioned transmission scheme, we set $\beta_n = 1$ to maximize the signal reflection by the IRS, i.e., $\Theta = \text{diag}(v_1, \dots, v_n, \dots, v_N)$ with $|v_n| = 1, n = 1, \dots, N$. In the following section, we derive the optimal throughput performance of the considered IRS-assisted user cooperation in WPCN.

III. THROUGHPUT PERFORMANCE ANALYSIS

A. Phase I: Energy Transfer

In the first stage of length t_1 , the HAP transmits energy with fixed power P_1 in t_1 amount of time. We denote the energy signal as $x_0(t)$ with $E[|x_0(t)|^2] = 1$. The signal received at WD_i can be expressed as [12]

$$y_i^{(1)}(t) = (\mathbf{g}\Theta_1\alpha_{iR} + \alpha_i)\sqrt{P_1}x_0(t) + n_i^{(1)}(t), i = 1, 2, \quad (2)$$

where $\Theta_1 = \text{diag}(v_{1,1}, \dots, v_{1,N})$ denotes the energy reflection coefficient matrix at the IRS with $|v_{1,n}| = 1$ for $n = 1, \dots, N$, $n_i^{(1)}(t)$ denotes the receiver noise. The amount of energy harvested by the i -th WD is given by

$$E_i = \eta E[|y_i^{(1)}(t)|^2]t_1 = \eta |\mathbf{g}\Theta_1\alpha_{iR} + \alpha_i|^2 P_1 t_1, i = 1, 2, \quad (3)$$

where $0 < \eta < 1$ denotes the fixed energy harvesting efficiency.¹

B. Phase II: Information Exchange

During the information exchange phase, WD_1 and WD_2 transmit their information to each other with the transmit power P_{21} and P_{22} for t_{21} and t_{22} amount of time, respectively. We denote $x_1(t)$ as the transmitted signal from WD_1

¹Although a single energy harvesting circuit exhibits non-linear energy harvesting property due to the saturation effect of circuit, it is shown that the non-linear effect can be effectively rectified by using multiple energy harvesting circuits concatenated in parallel, resulting in a sufficiently large linear conversion region in practice [17].

with $E[|x_1(t)|^2] = 1$. Then, the signal received at WD₂ and the HAP are expressed as, respectively,

$$y_2^{(2)}(t) = (\alpha_{2R}^T \Theta_2 \alpha_{1R} + \alpha_{12}) \sqrt{P_{21}} x_1(t) + n_2^{(2)}(t), \quad (4)$$

$$y_0^{(21)}(t) = (\mathbf{g} \Theta_2 \alpha_{1R} + \alpha_1) \sqrt{P_{21}} x_1(t) + n_0^{(2)}(t), \quad (5)$$

where $\Theta_2 = \text{diag}(v_{2,1}, \dots, v_{2,N})$ denotes the reflection-coefficient matrix at the IRS in duration t_{21} with $|v_{2,n}| = 1, n = 1, \dots, N$, $n_2^{(2)}(t)$ and $n_0^{(2)}(t)$ denote the receiver noise with power N_0 , $(\cdot)^T$ denotes the transpose operator. Then, the achievable rates from WD₁ to WD₂ and the HAP are

$$R_1^{(2)} = \frac{t_{21}}{T} \log_2 \left(1 + \frac{P_{21} |\alpha_{2R}^T \Theta_2 \alpha_{1R} + \alpha_{12}|^2}{N_0} \right), \quad (6)$$

$$R_0^{(21)} = \frac{t_{21}}{T} \log_2 \left(1 + \frac{P_{21} |\mathbf{g} \Theta_2 \alpha_{1R} + \alpha_1|^2}{N_0} \right). \quad (7)$$

Similarly, let $\Theta_3 = \text{diag}(v_{3,1}, \dots, v_{3,N})$ denote the reflection-coefficient matrix at the IRS when WD₂ transmits with duration t_{22} , where $|v_{3,n}| = 1, n = 1, \dots, N$. Then, the achievable rates from WD₂ to WD₁ and the HAP are

$$R_2^{(2)} = \frac{t_{22}}{T} \log_2 \left(1 + \frac{P_{22} |\alpha_{1R}^T \Theta_3 \alpha_{2R} + \alpha_{12}|^2}{N_0} \right), \quad (8)$$

$$R_0^{(22)} = \frac{t_{22}}{T} \log_2 \left(1 + \frac{P_{22} |\mathbf{g} \Theta_3 \alpha_{2R} + \alpha_2|^2}{N_0} \right). \quad (9)$$

C. Phase III: Joint Information Transmission

In the last phase of duration t_3 , the two WDs jointly transmit their information to the HAP. Meanwhile, the IRS reflects signal of the two WDs to the HAP. Specifically, WD_{*i*} transmits with power P_{3i} for t_{3i} amount of time for $i = 1, 2$. Thus, the total energy consumption of WD_{*i*} in Phase II and III is restricted by

$$t_{2i} P_{2i} + (t_{31} + t_{32}) P_{3i} \leq E_i, i = 1, 2. \quad (10)$$

In this stage, we consider Alamouti space-time block code transmit diversity scheme for joint information transmission, where the achievable rates from WD₁ and WD₂ to the HAP are

$$R_1^{(3)} = \frac{t_{31}}{T} \log_2 \left(1 + \frac{P_{31} |\mathbf{g} \Theta_4 \alpha_{1R} + \alpha_1|^2}{N_0} + \frac{P_{32} |\mathbf{g} \Theta_4 \alpha_{2R} + \alpha_2|^2}{N_0} \right), \quad (11)$$

$$R_2^{(3)} = \frac{t_{32}}{T} \log_2 \left(1 + \frac{P_{31} |\mathbf{g} \Theta_4 \alpha_{1R} + \alpha_1|^2}{N_0} + \frac{P_{32} |\mathbf{g} \Theta_4 \alpha_{2R} + \alpha_2|^2}{N_0} \right), \quad (12)$$

where $\Theta_4 = \text{diag}(v_{4,1}, \dots, v_{4,N})$ denotes the reflection-coefficient matrix at the IRS with $|v_{4,n}| = 1, n = 1, \dots, N$.

Overall, the achievable rate of WD_{*i*} is [7]

$$R_i = \min \left[R_i^{(2)}, R_0^{(2i)} + R_i^{(3)} \right], i = 1, 2. \quad (13)$$

Without loss of generality, we assume $T = 1$ in this paper.

IV. COMMON THROUGHPUT MAXIMIZATION

A. Problem Formulation

In this section, we focus on maximizing the common (minimum) throughput of the two WDs by jointly optimizing the transmit time allocation $\mathbf{t} = [t_1, t_{21}, t_{22}, t_{31}, t_{32}]$, power allocation $\mathbf{P} = [P_{21}, P_{22}, P_{31}, P_{32}]$ and the phase shift matrices $\tilde{\Theta} = [\Theta_1, \Theta_2, \Theta_3, \Theta_4]$, i.e.,

$$\begin{aligned} \text{(P1)} : \max_{\mathbf{t}, \mathbf{P}, \tilde{\Theta}} \quad & \min (R_1, R_2) \\ \text{s. t.} \quad & (1), (3) \text{ and } (10), \\ & t_1, t_{2i}, t_{3i}, P_{2i}, P_{3i} \geq 0, i = 1, 2, \\ & |v_{i,n}| = 1, i = 1, 2, 3, 4, n = 1, \dots, N. \end{aligned} \quad (14)$$

By introducing an auxiliary variable \bar{R} , (P1) can be equivalently rewritten as

$$\begin{aligned} \text{(P2)} : \quad & \max_{\bar{R}, \mathbf{t}, \mathbf{P}, \tilde{\Theta}} \quad \bar{R} \\ \text{s. t.} \quad & (1), (3) \text{ and } (10), \\ & t_1, t_{2i}, t_{3i}, P_{2i}, P_{3i} \geq 0, i = 1, 2, \\ & \bar{R} \leq R_1^{(2)}, \bar{R} \leq R_0^{(21)} + R_1^{(3)}, \\ & \bar{R} \leq R_2^{(2)}, \bar{R} \leq R_0^{(22)} + R_2^{(3)}, \\ & |v_{i,n}| = 1, i = 1, 2, 3, 4, n = 1, \dots, N. \end{aligned} \quad (15)$$

Notice that all the achievable data rates expressions of WD₁ and WD₂ are not concave functions. Besides, (3), (10) and the modulus constraint of $v_{i,n}$ are also not convex. Therefore, (P2) is a non-convex problem in its current form, which lacks of efficient optimal algorithms. In the next subsection, we transform the above non-convex problem into a convex one using semidefinite relaxation technique.

B. Proposed Solution to (P2)

To solve the non-convex problem (P2), let $\mathbf{v}_i = [v_{i,1}, \dots, v_{i,N}]$, $i = 1, 2, 3, 4$. Then, we have $\mathbf{g} \Theta_i \alpha_{jR} = \mathbf{v}_i \text{diag}(\mathbf{g}) \alpha_{jR}$, $j = 1, 2$, $\alpha_{2R}^T \Theta_2 \alpha_{1R} = \mathbf{v}_2 \text{diag}(\alpha_{2R}^T) \alpha_{1R}$ and $\alpha_{1R}^T \Theta_3 \alpha_{2R} = \mathbf{v}_3 \text{diag}(\alpha_{1R}^T) \alpha_{2R}$. To tackle the non-convex modulus constraint in (P2), we first define $\bar{\mathbf{v}}_i = \begin{bmatrix} \mathbf{v}_i^T \\ 1 \end{bmatrix}$, $i = 1, 2, 3, 4$, $\bar{\gamma}_j = \begin{bmatrix} \gamma_j \\ \alpha_j \end{bmatrix}$, $j = 1, 2$, $\bar{\gamma}_{2j} = \begin{bmatrix} \gamma_{2j} \\ \alpha_{12} \end{bmatrix}$, $\mathbf{V}_i = \bar{\mathbf{v}}_i \bar{\mathbf{v}}_i^H$, $\boldsymbol{\psi}_j = \bar{\gamma}_j \bar{\gamma}_j^H$ and $\boldsymbol{\psi}_{2j} = \bar{\gamma}_{2j} \bar{\gamma}_{2j}^H$, where $(\cdot)^H$ denotes the complex conjugate operator. Thus, we have

$$|\mathbf{g} \Theta_i \alpha_{jR} + \alpha_j|^2 = |\mathbf{v}_i \gamma_j + \alpha_j|^2 = \text{tr}(\mathbf{V}_i \boldsymbol{\psi}_j), \quad (16)$$

$$i = 1, 2, 3, 4, j = 1, 2,$$

$$|\alpha_{2R}^T \Theta_2 \alpha_{1R} + \alpha_{12}|^2 = |\mathbf{v}_2 \gamma_{21} + \alpha_{12}|^2 = \text{tr}(\mathbf{V}_2 \boldsymbol{\psi}_{21}), \quad (17)$$

$$|\alpha_{1R}^T \Theta_3 \alpha_{2R} + \alpha_{12}|^2 = |\mathbf{v}_3 \gamma_{22} + \alpha_{12}|^2 = \text{tr}(\mathbf{V}_3 \boldsymbol{\psi}_{22}), \quad (18)$$

where $\gamma_{21} = \text{diag}(\alpha_{2R}^T) \alpha_{1R}$, $\gamma_{22} = \text{diag}(\alpha_{1R}^T) \alpha_{2R}$ and $\gamma_j = \text{diag}(\mathbf{g}) \alpha_{jR}$, $j = 1, 2$.

Next, we introduce auxiliary variables $\tau_{2j} = t_{2j} P_{2j}$, $\tau_{3j} = t_{3j} P_{3j}$, $j = 1, 2$, $\tau'_{31} = t_{32} P_{31}$ and $\tau'_{32} = t_{31} P_{32}$. Note that $[\mathbf{V}_i]_{n,n} = 1, i = 1, 2, 3, 4, n = 1, \dots, N + 1$ hold from the

modulus constraint of $v_{i,n}$ ($[\mathbf{X}]_{m,n}$ denotes the element in the m -th row and n -th column of matrix \mathbf{X}). Then, we define $\mathbf{W}_1 = t_1 \mathbf{V}_1 \succeq 0$, $\mathbf{W}_2 = \tau_{21} \mathbf{V}_2 \succeq 0$, $\mathbf{W}_3 = \tau_{22} \mathbf{V}_3 \succeq 0$, $\mathbf{W}_{4j} = \tau_{3j} \mathbf{V}_4 \succeq 0$, $\mathbf{W}'_{4j} = \tau'_{3j} \mathbf{V}_4 \succeq 0$, $j = 1, 2$, which satisfy the following constraints

$$\begin{aligned} [\mathbf{W}_1]_{n,n} &= t_1, n = 1, \dots, N+1, \\ [\mathbf{W}_2]_{n,n} &= \tau_{21}, [\mathbf{W}_3]_{n,n} = \tau_{22}, \\ [\mathbf{W}_{4j}]_{n,n} &= \tau_{3j}, [\mathbf{W}'_{4j}]_{n,n} = \tau'_{3j}, j = 1, 2. \end{aligned} \quad (19)$$

Therefore, we can re-express $R_1^{(2)}$ in (6) as

$$\begin{aligned} R_1^{(2)} &= t_{21} \log_2 \left(1 + \rho \frac{|\mathbf{v}_2 \gamma_{21} + \alpha_{12}|^2 \tau_{21}}{t_{21}} \right), \\ &= t_{21} \log_2 \left(1 + \rho \frac{\text{tr}(\psi_{21} \mathbf{W}_2) \tau_{21}}{t_{21}} \right), \\ &= t_{21} \log_2 \left(1 + \rho \frac{\text{tr}(\psi_{21} \mathbf{W}_2)}{t_{21}} \right), \end{aligned} \quad (20)$$

where $\rho = \frac{1}{N_0}$ is a constant. Similarly, the achievable data rates in (7)-(9), (11) and (12) can be equivalently reformed as

$$R_0^{(21)} = t_{21} \log_2 \left(1 + \rho \frac{\text{tr}(\psi_1 \mathbf{W}_2)}{t_{21}} \right), \quad (21)$$

$$R_2^{(2)} = t_{22} \log_2 \left(1 + \rho \frac{\text{tr}(\psi_{22} \mathbf{W}_3)}{t_{22}} \right), \quad (22)$$

$$R_0^{(22)} = t_{22} \log_2 \left(1 + \rho \frac{\text{tr}(\psi_2 \mathbf{W}_3)}{t_{22}} \right), \quad (23)$$

$$R_1^{(3)} = t_{31} \log_2 \left(1 + \rho \frac{\text{tr}(\psi_1 \mathbf{W}_{41})}{t_{31}} + \rho \frac{\text{tr}(\psi_2 \mathbf{W}'_{42})}{t_{31}} \right), \quad (24)$$

$$R_2^{(3)} = t_{32} \log_2 \left(1 + \rho \frac{\text{tr}(\psi_1 \mathbf{W}'_{41})}{t_{32}} + \rho \frac{\text{tr}(\psi_2 \mathbf{W}_{42})}{t_{32}} \right). \quad (25)$$

Meanwhile, the energy constraint in (10) can be reformed as

$$\tau_{2j} + \tau_{3j} + \tau'_{3j} \leq \eta P_1 \text{tr}(\psi_j \mathbf{W}_1), i = 1, 2. \quad (26)$$

Notice that the achievable data rate $R_1^{(2)}$ in (20) is a concave function in (\mathbf{W}_2, t_{21}) , and similarly for the rate expressions in (21)-(25) (see the proof in [8]). Nonetheless, \mathbf{W}_1 needs to satisfy the non-convex constraint $\text{rank}(\mathbf{W}_1) = 1$, and so do $\mathbf{W}_2, \mathbf{W}_3, \mathbf{W}_{41}, \mathbf{W}'_{41}, \mathbf{W}_{42}$ and \mathbf{W}'_{42} . We denote $\boldsymbol{\tau} = [\tau_{21}, \tau_{22}, \tau_{31}, \tau'_{31}, \tau_{32}, \tau'_{32}]$ and $\widehat{\mathbf{W}} = [\mathbf{W}_1, \mathbf{W}_2, \mathbf{W}_3, \mathbf{W}_{41}, \mathbf{W}'_{41}, \mathbf{W}_{42}, \mathbf{W}'_{42}]$. We first drop the non-convex rank-one constraints and relax (P2) into the following problem,

$$\begin{aligned} \text{(P3)} : \quad & \max_{\bar{R}, t, \boldsymbol{\tau}, \widehat{\mathbf{W}}} \quad \bar{R} \\ \text{s. t.} \quad & t_1, t_{2j}, t_{3j}, \tau_{2j}, \tau_{3j}, \tau'_{3j} \geq 0, j = 1, 2, \\ & (1), (19) \text{ and } (26), \\ & \bar{R} \leq R_1^{(2)}, \bar{R} \leq R_0^{(21)} + R_1^{(3)}, \\ & \bar{R} \leq R_2^{(2)}, \bar{R} \leq R_0^{(22)} + R_2^{(3)}, \\ & \mathbf{W}_i, \mathbf{W}_{4j}, \mathbf{W}'_{4j} \succeq 0, i = 1, 2, 3, j = 1, 2. \end{aligned} \quad (27)$$

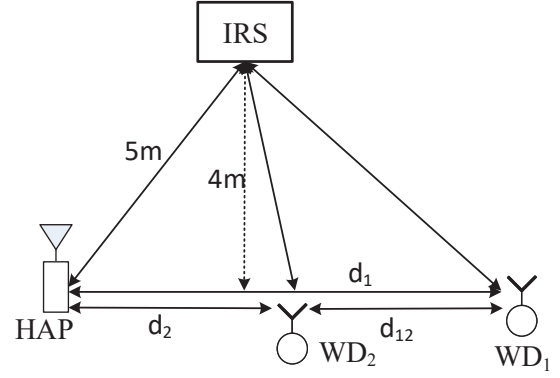


Fig. 2. The placement model of simulation setup.

(P3) is a standard semidefinite programming (SDP), which can be efficiently solved by convex tools such as CVX [18]. Let us denote the optimal solution to (P3) as $\{\bar{R}^*, t^*, \boldsymbol{\tau}^*, \widehat{\mathbf{W}}^*\}$, we can obtain the optimal $\mathbf{V}_1^* = \mathbf{W}_1^*/t_1^*$, $\mathbf{V}_2^* = \mathbf{W}_2^*/\tau_{21}^*$, $\mathbf{V}_3^* = \mathbf{W}_3^*/\tau_{22}^*$, $\mathbf{V}_4^* = \mathbf{W}_{41}^*/\tau_{31}^*$, $P_{2j}^* = \tau_{2j}^*/t_{2j}^*$, $P_{3j}^* = \tau_{3j}^*/t_{3j}^*$, $j = 1, 2$. However, the relaxed problem (P3) may not lead to a rank-one solution in general. Then, the Gaussian randomization method is employed to construct a rank-one solution. Specifically, to recover $\bar{\mathbf{v}}_1$ from \mathbf{V}_1^* , we obtain the eigenvalue decomposition of \mathbf{V}_1^* as $\mathbf{V}_1^* = \mathbf{U}\boldsymbol{\Sigma}\mathbf{U}^H$ [12], where $\mathbf{U} \in \mathbb{C}^{(N+1) \times (N+1)}$ and $\boldsymbol{\Sigma} \in \mathbb{C}^{(N+1) \times (N+1)}$ denote a unitary matrix and diagonal matrix, respectively. Then, we denote $\bar{\mathbf{v}}_1 = \mathbf{U}\boldsymbol{\Sigma}^{1/2}\mathbf{r}$ as a suboptimal solution, where $\mathbf{r} \in \mathbb{C}^{(N+1) \times 1}$ is a random vector generated according to $\mathbf{r} \sim \mathcal{CN}(\mathbf{0}, \mathbf{I}_{N+1})$. With independently generated Gaussian random vector, we select the optimal $\bar{\mathbf{v}}_1^*$ among all \mathbf{r} to achieve the maximum objective function value of (P3). Finally, we obtain $\mathbf{v}_1^* = e^{j \arg([\bar{\mathbf{v}}_1^*]_{(1:N)}/\bar{v}_{1,N+1}^*)}$, where $\arg(\cdot)$ denotes the phase extraction operation and $[\mathbf{a}]_{(1:N)}$ denotes the vector that contains the first N elements of \mathbf{a} . The optimal Θ_1^* can be obtained from \mathbf{v}_1^* . Following the similar procedure, we can recover \mathbf{v}_i^* , $i = 2, 3, 4$ from \mathbf{V}_i^* , and further obtain the optimal Θ_i^* from \mathbf{v}_i^* .

V. SIMULATION RESULTS

In this section, we provide simulation results to evaluate the performance of the proposed IRS-assisted cooperation scheme. To account for small-scale fading, we assume that all channels follow Rayleigh fading and the distance-dependent path loss is modeled as $L = C_0(\frac{d_i}{d_0})^{-\lambda}$, where $C_0 = 30$ dB is the path loss at the reference distance $d_0 = 1$ m, d_i , $i = 1, 2$, and d_{12} denote the HAP-WD $_i$ and WD $_1$ -WD $_2$ distance, and λ denotes the path loss exponent. To account for heterogeneous channel conditions, we set different path loss exponents of the HAP-IRS, IRS-WD $_i$, HAP-WD $_i$, WD $_1$ -WD $_2$ channels as 2.0, 2.2, 3.0, 3.0, respectively. Other required parameters are set as $P_1 = 30$ dBm, $\eta = 0.8$, and $N_0 = -80$ dBm. All the simulation results are obtained by averaging over 1000 channel

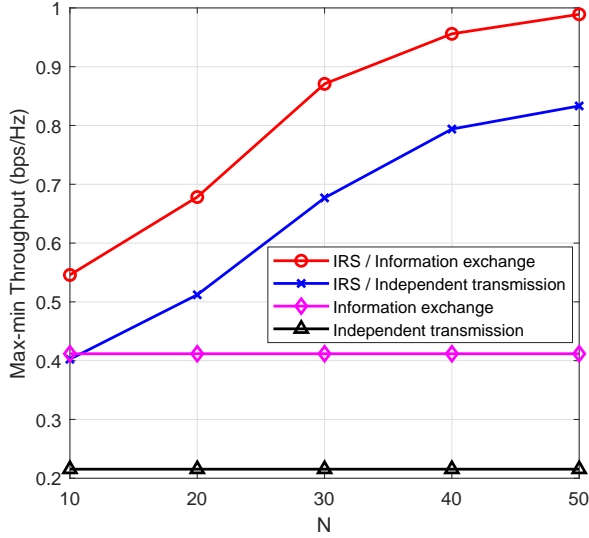


Fig. 3. The max-min throughput performance versus the number of reflecting elements N .

realizations. For performance comparison, we consider the following representative benchmark methods:

- 1) Independent transmission with IRS: This method follows the harvest-then-transmit protocol in [2]. Specifically, IRS is used to reflect RF energy from the HAP in the FL and WDs's information in the RL.
- 2) Information exchange without IRS: This corresponds to the two-user cooperation method in [6]. The detailed expressions are omitted here due to the page limit.
- 3) Independent transmission without IRS: WDs transmit their information independently in a round-robin manner to the HAP.

For fair comparison, we optimize the resource allocations in all the benchmark schemes, where the details are omitted due to the page limit.

We consider the placement model of the network system in Fig. 2. Fig. 3 first shows the impact of the numbers of reflecting elements N to the throughput performance. Without loss of generality, we set $d_1 = 8$ m, $d_2 = 5$ m and $d_{12} = 3$ m as a constant and change the value of N from 10 to 50. Obviously, the two IRS-assisted transmission methods achieve higher throughput due to the array gain. On average, the proposed IRS-assisted cooperation method achieves 30.17%, 102.23% and 275.11% higher throughput than the three benchmark methods, respectively.

Fig. 4 investigates the throughput performance versus the inter-user channel h_{12} . Here, we still use the placement model in Fig. 2, where we set $d_1 = 8$ m, $N = 20$ and vary d_{12} from 2 to 5 meters. Notice that the IRS-assisted communication methods always produce better performance than the other methods without IRS. We observe that the throughput of the independent transmission method is almost unchanged when d_{12} increases, because the performance bottleneck is

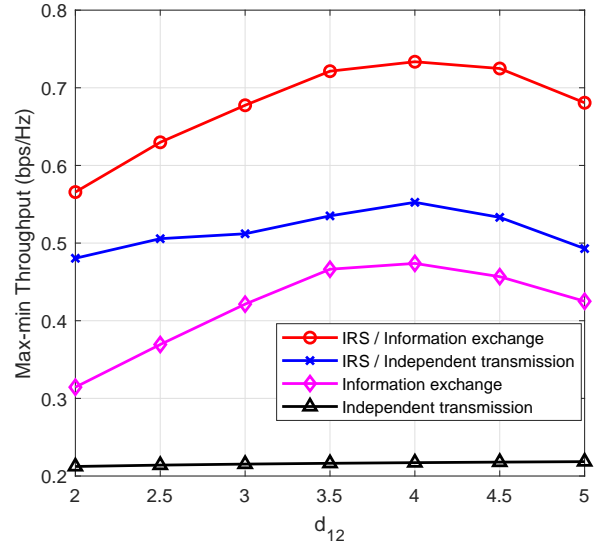


Fig. 4. The max-min throughput performance versus the inter-user channel.

the weak channel h_1 of the far user WD₁. It is observed that the throughput of the other three methods first increase when $d_{12} < 4$ m, but decrease as d_{12} further increases. This is because when WD₂ moves closer from the HAP and IRS, the signal gleaned from both the HAP and IRS become stronger. However, as we further increase d_{12} , the weak inter-user channel results in the degradation of the communication performance. Besides, the performance gap between the two IRS-assisted methods gradually increases with d_{12} . This shows that a weaker inter-user channel (larger d_{12}) leads to less efficient cooperation between the two users. Nonetheless, there exists significant performance gap between the two cooperation methods either with or without the use of IRS, indicating the effective performance enhancement of IRS in both energy and information transmissions.

Fig. 5 compares the achievable rate regions of three different schemes, i.e., the proposed IRS-assisted information exchange and independent transmission either with or without the assist of IRS. The rate region can be obtained by replacing the objective of problem (P1) with the weighted sum rate of the two users, i.e., $\omega R_1 + (1 - \omega)R_2$, and solve the optimization under different weighting factor ω from 0 to 1. The details are omitted due to the page limit. Similarly, we use the placement model in Fig. 2 with fixed $d_1 = 8$ m, $d_2 = 5$ m, $d_{12} = 3$ m and $N = 20$. Evidently, we see that the rate region of the proposed IRS-assisted cooperation method is significantly larger than that of the other two methods. On average, it achieves 25.59% and 57.98% higher throughput for WD₁, 45.99% and 102.04% higher throughput for WD₂ than the two benchmark methods, respectively. This indicates that the two users can benefit significantly both from the proposed cooperation and the use of IRS.

The simulation results in Fig. 3, Fig. 4 and Fig. 5 demon-

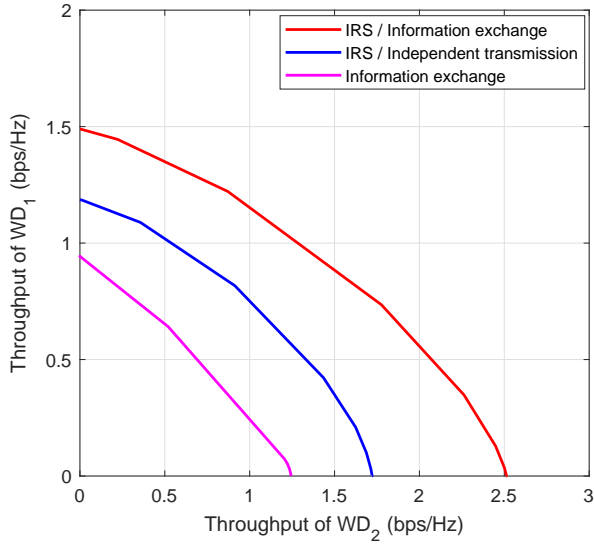


Fig. 5. The achievable rate region comparison of three different methods.

strate the advantage of applying the IRS to enhance the throughput performance both users when cooperation is considered in WPCN. Besides, the effective enhancement of energy efficiency and spectrum efficiency can benefit from the utilization of IRS.

VI. CONCLUSIONS

In this paper, we investigated the use of IRS in assisting the transmissions in a two-user cooperative WPCN. We formulated an optimization problem to maximize the common throughput. An efficient algorithm is proposed to jointly optimize the phase shifts of the IRS on reflecting the wireless energy and information signals, the transmission time and power allocation of the two WDs on wireless energy and information transmissions. Extensive simulations verified that the proposed IRS-assisted user cooperation method can effectively improve the throughput performance in WPCNs under different practical network setups.

REFERENCES

- [1] S. Bi, C. K. Ho, and R. Zhang, "Wireless powered communication: Opportunities and challenges," *IEEE Commun. Mag.*, vol. 53, no. 4, pp. 117-125, Apr. 2015.
- [2] H. Ju and R. Zhang, "Throughput maximization in wireless powered communication networks," *IEEE Trans. Wireless Commun.*, vol. 13, no. 1, pp. 418-428, Jan. 2014.
- [3] S. Bi and Y. J. Zhang, "Computation rate maximization for wireless powered mobile-edge computing with binary computation offloading," *IEEE Trans. Wireless Commun.*, vol. 17, no. 6, pp. 4177-4190, Jun. 2018.
- [4] L. Huang, S. Bi, and Y. J. Zhang, "Deep reinforcement learning for online computation offloading in wireless powered mobile-edge computing networks," *IEEE Trans. Mobile Comput.*, early access, doi: 10.1109/TMC.2019.2928811.
- [5] Y. Wu, L. Qian, H. Mao, X. Yang, and X. Shen, "Optimal power allocation and scheduling for non-orthogonal multiple access relay-assisted networks," *IEEE Trans. Mobile Comput.*, vol. 17, no. 11, pp. 2591-2606, Nov. 2018.

- [6] M. Zhong, S. Bi, and X. Lin, "User cooperation for enhanced throughput fairness in wireless powered communication networks," *Wireless Netw.*, vol. 23, no. 4, pp. 1315-1330, Apr. 2017.
- [7] H. Ju and R. Zhang, "User cooperation in wireless powered communication networks," in *Proc. IEEE GLOBECOM*, Austin, TX, USA, Dec. 2014, pp. 1430-1435.
- [8] Y. Zheng, S. Bi, X. Lin, and H. Wang, "Reusing wireless power transfer for backscatter-assisted relaying in WPCNs," *Comput. Netw.*, vol. 175, Jul. 2020, doi:10.1016/j.comnet.2020.107277.
- [9] L. Yuan, S. Bi, X. Lin, and H. Wang, "Optimizing throughput fairness of cluster-based cooperation in underlay cognitive WPCNs," *Comput. Netw.*, vol. 166, pp. 1-9, Jan. 2020.
- [10] T. J. Cui, M. Q. Qi, X. Wan, J. Zhao, and Q. Cheng, "Coding metamaterials, digital metamaterials and programmable metamaterials," *Light: Sci. Appl.*, vol. 3, no. 10, p. e218, Oct. 2014.
- [11] Q. Wu and R. Zhang, "Towards smart and reconfigurable environment: Intelligent reflecting surface aided wireless network," *IEEE Commun. Mag.*, vol. 58, no. 1, pp. 106-112, Jan. 2020.
- [12] Q. Wu and R. Zhang, "Intelligent reflecting surface enhanced wireless network via joint active and passive beamforming," *IEEE Trans. Wireless Commun.*, vol. 18, no. 11, pp. 5394-5409, Nov. 2019.
- [13] C. Huang, A. Zappone, G. C. Alexandropoulos, M. Debbah, and C. Yuen, "Reconfigurable intelligent surfaces for energy efficiency in wireless communication," *IEEE Trans. Wireless Commun.*, vol. 18, no. 8, pp. 4157-4170, Aug. 2019.
- [14] Q. Wu and R. Zhang, "Joint active and passive beamforming optimization for intelligent reflecting surface assisted SWIPT under QoS constraints," 2019. [Online]. Available: arxiv.org/abs/1910.06220.
- [15] Q. U. A. Nadeem, A. Kammoun, A. Chaaban, M. Debbah, and M. S. Alouini, "Asymptotic analysis of large intelligent surface assisted MIMO communications," 2019. [Online]. Available: arxiv.org/abs/1903.08127.
- [16] Y. Zheng, S. Bi, Y. J. Zhang, Z. Quan, and H. Wang, "Intelligent reflecting surface enhanced user cooperation in wireless powered communication networks," *IEEE Wireless Commun. Lett.*, vol. 9, no. 6, pp. 901-905, Jun. 2020.
- [17] J. M. Kang, I. M. Kim, and D. I. Kim, "Joint Tx power allocation and Rx power splitting for SWIPT system with multiple nonlinear energy harvesting circuit," *IEEE Wireless Commun. Lett.*, vol. 8, no. 1, pp. 53-56, Feb. 2019.
- [18] S. Boyd and L. Vandenberghe, *Convex Optimization*, Cambridge University Press, 2004.